

LETTER TO THE EDITOR

The Na D profiles of nearby low-power radio sources: jets powering outflows[★]

M. D. Lehnert¹, C. Tasse¹, N. P. H. Nesvadba², P. N. Best³, and W. van Driel¹

¹ GEPI, Observatoire de Paris, UMR 8111, CNRS, Université Paris Diderot, 5 place Jules Janssen, 92190 Meudon, France
e-mail: matthew.lehnert@obspm.fr

² Institut d'Astrophysique Spatiale, UMR 8617, CNRS, Université Paris-Sud, Bâtiment 121, 91405 Orsay Cedex, France

³ SUPA, Institute for Astronomy, Royal Observatory, Blackford Hill, Edinburgh EH9 3HJ, UK

Received 23 May 2011 / Accepted 2 July 2011

ABSTRACT

We have analyzed the properties of the Na D doublet lines at $\lambda\lambda 5890, 5896 \text{ \AA}$ in a large sample of 691 radio galaxies using the Sloan Digital Sky Survey (SDSS). These radio galaxies are resolved in the FIRST survey, have redshifts less than 0.2 and radio flux densities at 1.4 GHz higher than 40 mJy. The sample is complete within the main spectroscopic magnitude limits of the SDSS. Approximately 1/3 of the sources show a significant excess (above that contributed by their stellar populations) of Na D absorption that can be robustly fitted with two Voigt profiles representing the Na D doublet. A further 1/6 of the sources show residual absorption, for which the fits were not well constrained though while $\sim 50\%$ of the sample show no significant residual absorption. The residual absorption is modestly blueshifted, typically by $\sim 50 \text{ km s}^{-1}$, but the velocity dispersions are high, generally $\sim 500 \text{ km s}^{-1}$. Assuming that the size of the absorbing region is consistent with $\sim 1 \text{ kpc}$ for dust lanes in a sample of generally more powerful radio sources, assuming a continuous constant velocity flow (continuity equation), we estimate mass and energy outflow rates of about $10 M_{\odot} \text{ yr}^{-1}$ and $\text{few} \times 10^{42} \text{ erg s}^{-1}$. These rates are consistent with those in the literature based on H I absorption line observations of radio galaxies. The energy required to power these outflows is on the order of 1–10% of the jet mechanical power and we conclude that the radio jet alone is sufficient. The mass and energy outflow rates are consistent with what is needed to heat/expel the mass returned by the stellar populations as well as the likely amount of gas from a cooling halo. This suggests that radio-loud AGN play a key role in energizing the outflow/heating phase of the feedback cycle. The deposition of the jet mechanical energy could be important for explaining the ensemble characteristics of massive early type galaxies in the local universe.

Key words. galaxies: evolution – galaxies: ISM – galaxies: jets – galaxies: kinematics and dynamics

1. Introduction

The self-limiting cycle whereby the fueling of a supermassive black hole regulates both the rate at which it is fueled and the rate at which the surrounding spheroid grows – the feedback from active galactic nuclei (AGN feedback) – is engendering a substantial legacy in theoretical astrophysics. This cycle is invoked to explain many things, from why massive early type galaxies are “old, red, and dead” and their evolutionary behavior appears “anti-hierarchical” (e.g.; Thomas et al. 2005; Best et al. 2005b, 2006), the relationship between the masses of black holes and bulges (Tremaine et al. 2002), the “entropy floor” and lack of cooling flows in the inter-cluster medium (ICM; e.g.; Fang & Haiman 2008; Rafferty et al. 2008) and preventing the cooling of gas from the evolving stellar population (Ciotti et al. 2009), plus a seeming plethora of other characteristics of nearby galaxies, their halos, ICM and inter-galactic medium.

Despite its potential importance, AGN feedback has remained in the realm of theoretical *deus ex machina* processes. This is mainly because it is difficult to obtain the necessary observations that may tell us how AGN feedback regulates both the growth of the black hole and the galaxy. Here, we focus on radio sources because their mechanical energy output can be estimated, allowing us to gauge whether jets are a viable,

though perhaps not the only, mechanism for creating the necessary feedback cycle. Best et al. (2005b) demonstrated that 30% of all nearby, early-type galaxies more luminous than L^* in the SDSS have radio-loud AGN, and subsequently argued that this mechanical energy output could balance cooling of the X-ray gas (Best et al. 2006). Powerful radio sources, based on energetic and (and in some cases) morphological arguments, appear capable of driving energetic outflows of gas, which encompass a large number of phases including molecular (Fischer et al. 2010), warm ionized (e.g. Fu & Stockton 2009; Holt et al. 2008; Nesvadba et al. 2008; Fischer et al. 2011), and warm neutral gas (e.g. Morganti et al. 2005a,b, 2007).

Absorption lines provide a robust way of probing one half of the feedback cycle. Because absorption lines are seen projected against the emission from the galaxy, negative radial velocities relative to systemic are an unambiguous sign of outflows. Most of the strong resonance lines of cosmically abundant ions are found in the UV (e.g., Morton 1991; Savage & Sembach 1996), and so must be studied from space, with, e.g., HST or FUSE. In the present study we have instead opted to exploit the vast data set of the SDSS to study a large sample of radio galaxies using the Na I doublet at $\lambda\lambda 5890, 5896 \text{ \AA}$, optical absorption lines that present another way of probing outflows from AGN. The ionization potential of Na I is only 5.1 eV, corresponding to a wavelength of $\lambda \sim 2420 \text{ \AA}$, which is less than that of hydrogen.

[★] Figure 3 is available in electronic form at
<http://www.aanda.org>

This implies that the photons that ionize Na I are in the near-UV and that sodium is mainly shielded from ionizing radiation by dust. These lines therefore primarily probe the dusty warm atomic phase and the cold molecular phase (Spitzer 1978).

For Na D lines to be observed, only relatively modest optical depths and H I column densities are required, which makes them a sensitive probe of the outflowing (or inflowing) neutral ISM. To observe the lines, the extinction must be sufficient for $\tau \gtrsim 1$ at 2420 Å, which corresponds to $A_V = 0.43$ mag in the V-band for a Cardelli et al. (1989) extinction law and a selective extinction of $R_V = 3.1$ and to an H I column density of $8 \times 10^{20} \text{ cm}^{-2}$.

2. Sample and methodology

The target sample is drawn from the seventh data release of the SDSS survey. All galaxies with spectroscopic redshifts were cross-matched with the NVSS and FIRST radio surveys following the techniques outlined in Best et al. (2005a). All sources have a 1.4 GHz flux density (from FIRST and NVSS) exceeding 40 mJy, i.e., more than an order of magnitude less than those observed in H I (Morganti et al. 2007, 2005a,b). All galaxies have been visually inspected to ensure secure detections, and their radio morphologies have been classified. The NaD sample consists of all 691 of these SDSS galaxies that have redshift $z < 0.2$ and an extended radio morphology at the ≈ 5 arcsec resolution of the FIRST survey. We have focused on radio sources with extended morphologies because in these the jet mechanical power can be robustly estimated (Cavagnolo et al. 2010).

To estimate the contribution of any Na I in the interstellar medium of the host galaxies, we first had to remove the stellar contribution to the absorption lines by fitting each SDSS spectrum with a linear combination of stellar population models taken from Bruzual & Charlot (2003) using the publicly available code STARLIGHT (Cid Fernandes et al. 2005). The regions of strong emission lines and those around the Na D lines were excluded from the fits. All spectra were well fitted and had reduced χ^2 values, suggesting the fits were highly significant.

After removing the stellar continuum in the normalized spectra, we fitted both lines of the Na D doublet in a 100 Å wide region surrounding them, using a minimization routine and assuming the lines are represented by a Voigt profile with the appropriate atomic parameters (Morton 2003). About half the sample did show significant Na D absorption line residuals, in fits that were robust based on their χ^2_ν values. However, because of the subtraction of the stellar contribution of the lines, about 1/6 of the fits to the sources with significant residual absorption were not well constrained. This manifested itself most obviously when the core of the line was not deep compared to the overall rms noise level of the residual spectrum. We therefore adopted a threshold on the greatest depth of the lines to be used for further analysis of about 5 times the rms of the residual spectrum. This is conservative, in that some of the sources with line cores weaker than this do show Na D absorption residuals. But given the reasonably large range of possible widths and offset velocities for such sources, we feel it is prudent to exclude them from the analysis (we refer to these sources as “unconstrained” for the sake of brevity). Furthermore, because the He I line at 5875.6 Å overlaps with the blue wings of the (broad) Na D lines, our desire to obtain robust results made us exclude all 14 galaxies with strong He I emission. Thus, overall, about 1/3 of all the sources had significant Na D residuals that had fits that were well constrained. The fit parameters are the line core depth, dispersion, and the velocity offset relative to the systemic velocity (based

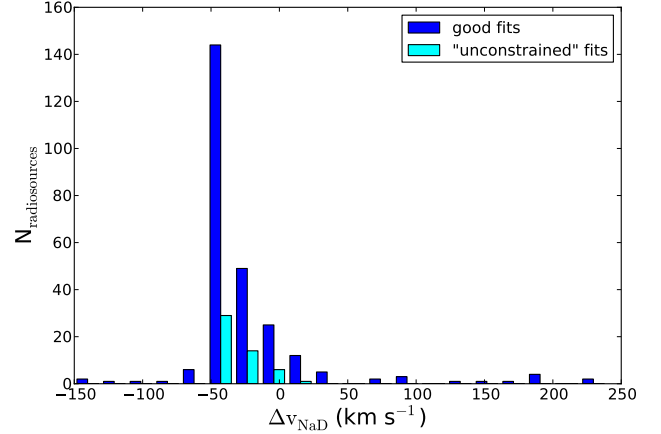


Fig. 1. Distribution of fitted NaD absorption line offset velocities for our sample of radio sources. The classification of fit qualities is indicated in the figure legend.

on the redshifts determined from other stellar absorption lines in the spectrum). In all cases, the lines were sufficiently broad for the doublet not to be resolved into two distinct components.

Na I, our gas kinematics tracer, is a minor constituent of the warm neutral medium, most of which is in H I. To estimate the column density of H I relative to Na I, we require a Na depletion factor for atoms lost on grains, an ionization correction and a Na/H abundance ratio. While we cannot determine these quantities directly, if we assume the clouds were similar to what is observed in the Milky Way, with a solar Na to H abundance ratio (-5.70 in the log), then the depletion on grains is likely to be about a factor of a few and the ionization correction about 100 (Phillips et al. 1984). However, there is a weak trend of decreasing Na abundance with increasing column density (Wakker & Mathis 2000), and over the range of likely H I column densities in our targets, the Na I column densities are a few hundred times lower (Wakker & Mathis 2000, and reference therein). Based on these estimates, we have adopted a ratio of ~ 460 to account for depletion and ionization correction.

3. Results

In our sample of nearly 700 radio-loud early-type galaxies at $z < 0.2$, with 1.4 GHz flux densities above 40 mJy, about 1/3 (260) of the sources show a significant detection of the Na D doublet in absorption, whereas half (362) the sample do not. We probed column densities $\log N_{\text{NaI}} (\text{cm}^{-2}) \approx 11.5\text{--}13.5$, which, not surprisingly, are about the level necessary to provide $\tau_{\text{dust}} = 1$ at 2420 Å (5.1 eV). Converting our estimate of Na I column densities to H I (using the Milky Way-like conversion factors given in Sect. 2), $\log N_{\text{HI}} (\text{cm}^{-2}) \sim 20\text{--}22$ similar to what is probed in H I (Morganti et al. 2003, 2005a,b). The velocity offsets are relatively small, $\lesssim 200 \text{ km s}^{-1}$, and even positive for a handful of sources (Fig. 1). The velocity dispersions, σ_{NaD} , are typically $\sim 500\text{--}600 \text{ km s}^{-1}$ (Fig. 2).

Our goal is to understand the energy and mass outflow rates that may, or may not, be driven by the radio jet. Key to this analysis is the robustness of our fits. We therefore constructed a Monte Carlo simulation that creates a series of artificial lines with the same characteristics as the observed sample, which were then fitted in the same way as the data. For this, we simply assumed either (1) a constant value for both the covering fraction and the column density (both quantities were varied between simulations) and varying signal-to-noise ratios, velocity offsets

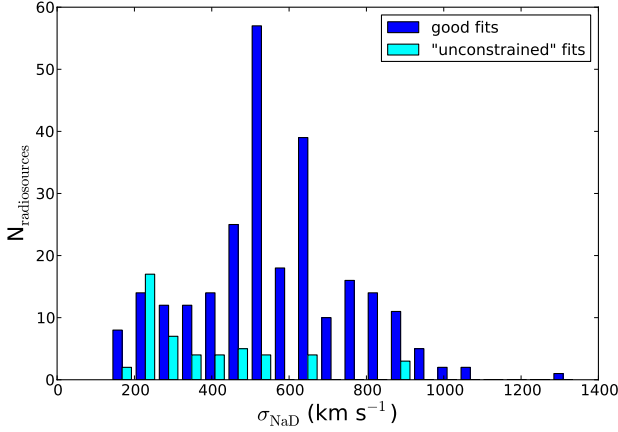


Fig. 2. Distribution of NaD absorption line velocity dispersions for our sample of radio sources. The classification of fit qualities is indicated in the figure legend.

and dispersions according to a uniform distribution with ranges like those obtained from the data, or (2) that all quantities are uniformly distributed, similar to the range of values observed. Our fits to the observed data show a trend between the covering fraction, C_f , and the column density, N_{NaD} (Fig. 3), and we needed our robustness simulations to assess if this is an artifact of the fitting or if it has an astrophysical cause. What we found (especially from the simulations where we kept the column density and covering fraction constant) was that we can reproduce the characteristics of the relationship between C_f and N_{NaD} . At high values for both N_{NaD} (well above 10^{13} cm^{-2}) and covering fractions (above about a few tenths), the fits are robust, do not show a particular strong correlation between C_f and N_{NaD} , and reproduce the input distribution of the dispersion and velocity offset. It is in the lower column and/or lower covering fraction regimes that we see this correlation, which is purely artificial. This is simply because the depth of the line is a function of C_f , σ_{NaD} and N_{NaD} , with different dependences if the lines are saturated or not. When the line is not (strongly) saturated, C_f and N_{NaD} are highly degenerate.

The most robust quantities we found for a good recovery of our input distributions were the dispersion, velocity offsets, and the product $C_f \times N_{\text{NaD}}$. The latter is important because the energy and mass outflow estimates depend on the combination of these quantities. The input distribution of the dispersions is generally recovered, and only the number of galaxies with high dispersions are slightly underestimated (the recovered means were robust). The combination of $C_f \times N_{\text{NaD}}$ is recovered statistically to within a factor of ~ 2 . For example, if we assume a constant combination of $C_f = 0.5$ and $N_{\text{NaD}} = 3 \times 10^{13} \text{ cm}^{-2}$, and uniform distributions for the dispersions, velocity offset and S/N, we find that the resulting product, $C_f N_{\text{NaD}}$, has a mean of $1.5 \times 10^{13} \text{ cm}^{-2}$ and that 68% of the data are between $0.5\text{--}3 \times 10^{13} \text{ cm}^{-2}$ – i.e., a majority of the values lie within a factor of about 2 (the results are shown in Fig. 3).

4. Discussion and conclusions

We can estimate the outflow rates of mass, \dot{M} , and energy, \dot{E} , in these galaxies by assuming that the continuity equation for mass and energy applies. For a spherical, continuous gas outflow with a covering fraction C_f , H I column density N_{HI} , wind opening angle Ω , flowing through a radius r , and having a constant velocity

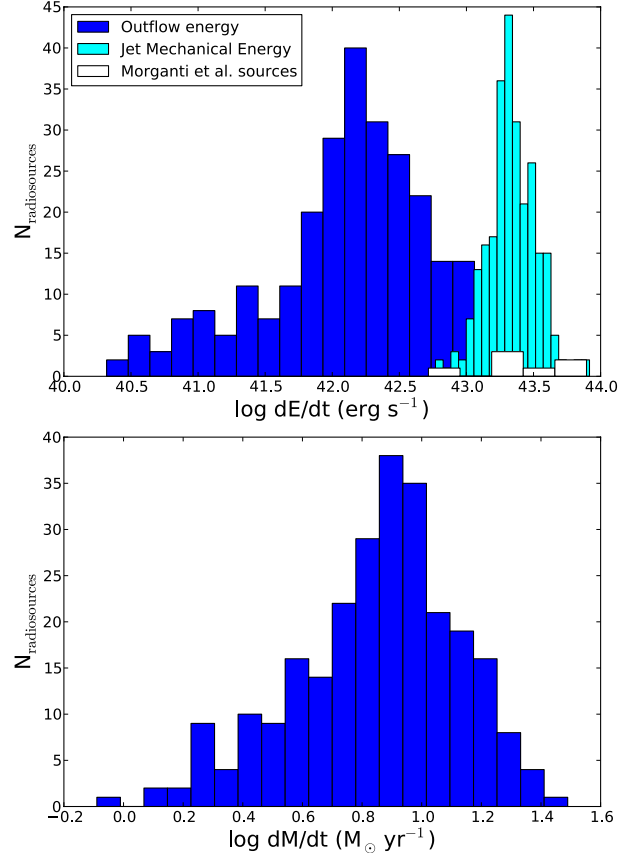


Fig. 4. Blue histograms show the energy (*top*) and mass (*bottom*) outflow rates estimated for our sources with robust NaD detections, given a flow radius of 1 kpc for all sources. The estimated jet mechanical power is represented by the aqua histogram in the top panel, which can be compared with that of radio sources with H I absorption detections (white; Morganti et al. 2005a). The jet power estimates would be about an order of magnitude greater if we used the relationship from Cavagnolo et al. (2010).

equal to that observed, the continuity equation implies (e.g. Heckman et al. 2000)

$$\begin{aligned} \dot{M} &\sim 60 (r/\text{kpc})(N_{\text{H}}/3 \times 10^{21} \text{ cm}^{-2})(\delta v/200 \text{ km s}^{-1})(\Omega/4\pi)C_f \quad (1) \\ \dot{E} &\sim 8 \times 10^{41} (r/\text{kpc})(N_{\text{H}}/3 \times 10^{21} \text{ cm}^{-2})(\delta v/200 \text{ km s}^{-1})^3 \\ &\quad \times (\Omega/4\pi)C_f \quad (2) \end{aligned}$$

The observed frequency of significant Na D absorption is strongly influenced by the opening angle (because the background against which the absorption line is seen is large), whereas C_f influences (mostly) the depth of the line. In addition, to obtain a more adequate representation of the terminal velocity of the Na D lines, we have assumed that δv is not the measured offset velocity but rather the geometric combination of the offset velocity and the line dispersion. Given the range of values, the terminal velocities are on the order of 1000 km s^{-1} (see also Morganti et al. 2005a).

De-acceleration of the radio jet and shock heating of the inhomogeneous circum-nuclear gas transfers both momentum and energy from the jet to the ambient ISM (e.g., the numerical simulations of Wagner & Bicknell 2011). An energy-driven bubble develops, which rapidly expands and further accelerates additional gas and ISM clouds (Sutherland & Bicknell 2007; Wagner & Bicknell 2011). Because we cannot directly measure the radii over which the energy-driven bubble is entraining and accelerating clouds in any individual source, we must estimate these radii in a more circuitous manner.

Most of the mass that is accelerated is located where the gas and cloud density is the highest – within the inner \sim kpc. Clouds in the ISM are accelerated very quickly ($\lesssim 10^7$ yr) to high velocities, and over relatively small radii only (\lesssim kpc), as shown in numerical simulations by, e.g., [Wagner & Bicknell \(2011\)](#). Of course, while these clouds accelerate away from the AGN, they are heated, ionized and destroyed by mechanical and thermal instabilities ([Nakamura et al. 2006](#)). We have also argued that because of the low ionization potential of Na, Na D absorption must be sampling dusty clouds in the warm atomic and cold molecular phases of the ISM. Therefore, we adopted 1 kpc for the radius the absorbing material is flowing through, this being the average angular size of the dust lanes in the 3CR radio sample imaged by HST ([de Koff et al. 2000](#)). Because the probable 1 kpc size of the dust lanes is much smaller than the average 7 kpc projected size of the SDSS spectroscopic fiber, this favors a small covering fraction for the Na D absorption and therefore high column densities. The absorption is likely dominated by clouds that have high column densities ($\sim 10^{21-22}$ cm $^{-2}$) but a low covering fraction ($\sim 10\%$) of the optical continuum light from the host galaxy.

We find that the mass and energy outflow rates are about $10 M_{\odot}$ yr $^{-1}$ and a few $\times 10^{42}$ erg s $^{-1}$, respectively. Our sources have an average and median radio luminosity at 1.4 GHz of 10^{25} W Hz $^{-1}$ and $10^{24.6}$ W Hz $^{-1}$, respectively. The mechanical energy from the jet can be estimated using a scaling relationship with the 1.4 GHz luminosity. Adopting the one given in [Best et al. \(2006\)](#), and references therein) yields a typical mechanical energy of our sources of $\sim 2 \times 10^{43}$ erg s $^{-1}$ (Fig. 4), while the relationship from [Cavagnolo et al. \(2010\)](#) gives estimates that are about one order of magnitude greater (this difference in energy estimates is mainly due to differing assumptions about the work done in inflating the X-ray cavities observed in clusters). Given the order-of-magnitude spirit of these estimates, it appears that about 1–10% of the jet mechanical energy is needed to power these outflows. This modest requirement implies that it is quite plausible for the jet itself to provide the required power. A similar conclusion based on X-ray cooling arguments was also drawn by [Best et al. \(2006\)](#). We do not find a correlation between the energy of the outflow and the jet mechanical energy. This is likely owing to the crudeness of our estimates but also to real astrophysical effects such as the coupling efficiency of the jet mechanical energy to the ISM, the relative direction of the jet compared to the distribution of the ISM, the range of masses of the warm neutral medium in these galaxies, etc.

The mass outflow rates derived in this analysis are similar to those estimated for radio sources in H I ([Morganti et al. 2005a,b](#)). This is not surprising given the similarity in approximate jet mechanical energies of the two samples (Fig. 4). Over a plausible lifetime of 10^{7-8} yr, an extended radio source will drive out/heat about $10^{8-9} M_{\odot}$ of gas and inject about 10^{57-58} erg of energy. This estimate can be compared with the rate at which the stellar populations return gas to the ISM of their galaxies and the total binding energy of the galaxy. A massive (stellar masses $\approx 10^{11} M_{\odot}$) evolved (~ 10 Gyr) galaxy will return about $1 M_{\odot}$ yr $^{-1}$ (e.g. [Mathews & Brighenti 2003](#)). While we do not know how much gas the jet will remove from the potential of the galaxy, our estimated mass and energy outflow rates are substantial compared to both the total amount of ISM in the typical elliptical, $10^9 M_{\odot}$ (which is mostly in X-ray emitting gas), the rate of return from the stellar population, and amounts to

virtually the binding energy of a massive galaxy over the lifetime of the AGN.

In massive galaxies, [Best et al. \(2005b\)](#) found at the radio luminosities spanned by our sample that about a few to 10% have active radio sources. This either suggests that the lifetimes of radio-loud AGN are very long (which is unlikely) or that the duty cycle of AGN is high. If the lifetimes are as short as 10^8 yr, this implies that the inactive phase lasts for only a few 100 Myr, during which period it is likely that the host would accumulate an additional $10^{8-9} M_{\odot}$ of gas if most of it were caused by mass loss from stars within the galaxy. This amount is again similar to what the radio source will heat during its lifetime (see [Best et al. 2006](#), for more details). From these rough estimates we conclude that the AGN is powering at least half of the necessary feedback cycle – the outflow/heating phase. More observations and better modeling are needed to constrain the whole cycle of AGN feedback (e.g. [Nesvadba et al. 2010](#)).

Acknowledgements. The work of C.T. is supported by a grant from the Agence Nationale de la Recherche (ANR) in France. We thank the anonymous referee for helpful criticisms.

References

- Best, P. N., Kauffmann, G., Heckman, T. M., et al. 2005a, MNRAS, 362, 25
 Best, P. N., Kauffmann, G., Heckman, T. M., & Ivezić, Ž. 2005b, MNRAS, 362, 9
 Best, P. N., Kaiser, C. R., Heckman, T. M., & Kauffmann, G. 2006, MNRAS, 368, L67
 Bruzual, G., & Charlot, S. 2003, MNRAS, 344, 1000
 Cardelli, J. A., Clayton, G. C., & Mathis, J. S. 1989, ApJ, 345, 245
 Cavagnolo, K. W., McNamara, B. R., Nulsen, P. E. J., et al. 2010, ApJ, 720, 1066
 Cid Fernandes, R., Mateus, A., Sodré, L., Stasińska, G., & Gomes, J. M. 2005, MNRAS, 358, 363
 Ciotti, L., Ostriker, J. P., & Proga, D. 2009, ApJ, 699, 89
 de Koff, S., Best, P., Baum, S. A., et al. 2000, ApJS, 129, 33
 Fang, W., & Haiman, Z. 2008, ApJ, 680, 200
 Fu, H., & Stockton, A. 2009, ApJ, 690, 953
 Fischer, J., Sturm, ãE., González-Alfonso, E., et al. 2010, A&A, 518, L41
 Fischer, T. C., Crenshaw, D. M., Kraemer, S. B., et al. 2011, ApJ, 727, 71
 Gaibler, V., Krause, M., & Camenzind, M. 2009, MNRAS, 400, 1785
 Heckman, T. M., Lehnert, M. D., Strickland, D. K., & Armus, L. 2000, ApJS, 129, 493
 Holt, J., Tadhunter, C. N., & Morganti, R. 2008, MNRAS, 387, 639
 Mathews, W. G., & Brighenti, F. 2003, ApJ, 590, L5
 Morganti, R., Oosterloo, T. A., Emonts, B. H. C., van der Hulst, J. M., & Tadhunter, C. N. 2003, ApJ, 593, L69
 Morganti, R., Tadhunter, C. N., & Oosterloo, T. A. 2005a, A&A, 444, L9
 Morganti, R., Oosterloo, T. A., Tadhunter, C. N., van Moorsel, G., & Emonts, B. 2005b, A&A, 439, 521
 Morganti, R., Holt, J., Saripalli, L., Oosterloo, T. A., & Tadhunter, C. N. 2007, A&A, 476, 735
 Morton, D. C. 1991, ApJS, 77, 119
 Morton, D. C. 2003, ApJS, 149, 205
 Nakamura, F., McKee, C. F., Klein, R. I., & Fisher, R. T. 2006, ApJS, 164, 477
 Nesvadba, N. P. H., Lehnert, M. D., De Breuck, C., Gilbert, A. M., & van Breugel, W. 2008, A&A, 491, 407
 Nesvadba, N. P. H., Boulanger, F., Salomé, P., et al. 2010, A&A, 521, A65
 Phillips, A. P., Pettini, M., & Gondhalekar, P. M. 1984, MNRAS, 206, 337
 Rafferty, D. A., McNamara, B. R., & Nulsen, P. E. J. 2008, ApJ, 687, 899
 Savage, B. D., & Sembach, K. R. 1996, ARA&A, 34, 279
 Spitzer, L. 1978, Physical processes in the interstellar medium (Wiley-Interscience, New York)
 Sutherland, R. S., & Bicknell, G. V. 2007, ApJS, 173, 37
 Thomas, D., Maraston, C., Bender, R., & Mendes de Oliveira, C. 2005, ApJ, 621, 673
 Tremaine, S., Gebhardt, K., Bender, R., et al. 2002, ApJ, 574, 740
 Wagner, A. Y., & Bicknell, G. V. 2011, ApJ, 728, 29
 Wakker, B. P., & Mathis, J. S. 2000, ApJ, 544, L107

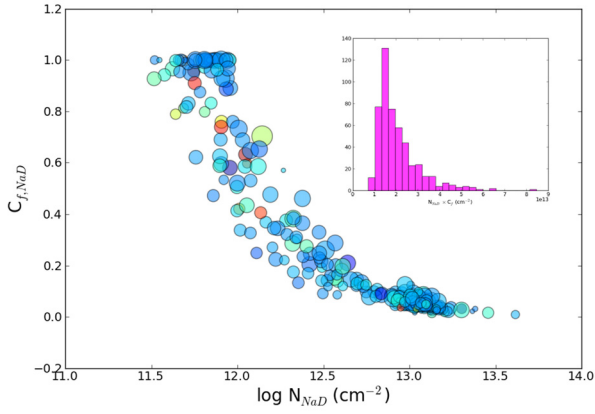


Fig. 3. Relationship between the fitted column density of Na, N_{NaD} , and the covering fraction, C_f , of the best-fit model for the Na D lines. The color and size of each circle is related to the velocity offset (purple to red indicates -100 to $+200 \text{ km s}^{-1}$) and dispersion of the lines (lowest to highest indicates 200 to $\sim 1000 \text{ km s}^{-1}$) respectively. This trend is artificially induced because the individual components of the doublet are not resolved and does not affect the overall results. The inset (magenta histogram) shows the distribution of $N_{\text{NaD}} \times C_f$ from the Monte-Carlo simulations, where the column density and covering fractions were held constant at $3 \times 10^{13} \text{ cm}^{-2}$ and 0.5 respectively (see text for details).